



**EUROfusion**

EUROFUSION WPMST2-PR(16) 15224

DE Aguiam et al.

**Implementation of the new multichannel  
X-mode edge density profile  
reflectometer for the ICRF antenna on  
ASDEX Upgrade**

Preprint of Paper to be submitted for publication in  
21st Topical Conference on High Temperature Plasma  
Diagnostics 2016



This work has been carried out within the framework of the EUROfusion Consortium and has received funding from the Euratom research and training programme 2014-2018 under grant agreement No 633053. The views and opinions expressed herein do not necessarily reflect those of the European Commission.

This document is intended for publication in the open literature. It is made available on the clear understanding that it may not be further circulated and extracts or references may not be published prior to publication of the original when applicable, or without the consent of the Publications Officer, EUROfusion Programme Management Unit, Culham Science Centre, Abingdon, Oxon, OX14 3DB, UK or e-mail [Publications.Officer@euro-fusion.org](mailto:Publications.Officer@euro-fusion.org)

Enquiries about Copyright and reproduction should be addressed to the Publications Officer, EUROfusion Programme Management Unit, Culham Science Centre, Abingdon, Oxon, OX14 3DB, UK or e-mail [Publications.Officer@euro-fusion.org](mailto:Publications.Officer@euro-fusion.org)

The contents of this preprint and all other EUROfusion Preprints, Reports and Conference Papers are available to view online free at <http://www.euro-fusionscipub.org>. This site has full search facilities and e-mail alert options. In the JET specific papers the diagrams contained within the PDFs on this site are hyperlinked

# Implementation of the new multichannel X-mode edge density profile reflectometer for the ICRF antenna on ASDEX Upgrade<sup>a)</sup>

D.E. Aguiam,<sup>1, b)</sup> A. Silva,<sup>1</sup> V. Bobkov,<sup>2</sup> P.J. Carvalho,<sup>1</sup> P.F. Carvalho,<sup>1</sup> R. Cavazzana,<sup>3</sup> G.D. Conway,<sup>2</sup> O. D'Arcangelo,<sup>4</sup> L. Fattorini,<sup>5</sup> H. Faugel,<sup>2</sup> A. Fernandes,<sup>1</sup> H. Fünfgelder,<sup>2</sup> B. Goncalves,<sup>1</sup> L. Guimaraes,<sup>1</sup> G. De Masi,<sup>3</sup> L. Meneses,<sup>1</sup> J.M. Noterdaeme,<sup>2, 6</sup> R.C. Pereira,<sup>1</sup> G. Rocchi,<sup>4</sup> J.M. Santos,<sup>1</sup> A.A. Tuccillo,<sup>4</sup> O. Tudisco,<sup>4</sup> and ASDEX Upgrade Team<sup>2</sup>

<sup>1)</sup> Instituto de Plasmas e Fusão Nuclear, Instituto Superior Técnico, Universidade de Lisboa, 1049-001 Lisboa, Portugal

<sup>2)</sup> Max-Planck-Institut für Plasmaphysik, Boltzmannstr. 2, D-85748 Garching, Germany

<sup>3)</sup> Consorzio RFX (CNR, ENEA, INFN, Università di Padova, Acciaierie Venete SpA), Corso Stati Uniti 4, 35127 Padova, Italy

<sup>4)</sup> ENEA, Dipartimento FSN, C. R. Frascati, via E. Fermi 45, 00044 Frascati (Roma), Italy

<sup>5)</sup> Università degli Studi Milano Bicocca, dipartimento di Fisica, piazza della Scienza 3, 20126 Milano, Italy

<sup>6)</sup> Ghent University, Applied Physics Department, B-9000 Gent, Belgium

(Dated: 30 May 2016)

A new multichannel frequency modulated continuous-wave reflectometry diagnostic has been successfully installed and commissioned on ASDEX Upgrade to measure the plasma edge electron density profile evolution in front of the Ion Cyclotron Range of Frequencies (ICRF) antenna. The design of the new three-strap ICRF antenna integrates ten pairs (sending and receiving) of microwave reflectometry antennas. The multichannel reflectometer can use three of these to measure the edge electron density profiles up to  $2 \times 10^{19} \text{ m}^{-3}$ , at different poloidal locations, allowing the direct study of the local plasma layers in front of the ICRF antenna. ICRF power coupling, operational effects and poloidal variations of the plasma density profile can be consistently studied for the first time. In this work the diagnostic hardware architecture is described and the obtained density profile measurements were used to track outer radial plasma position and plasma shape.

## I. INTRODUCTION

The operation and coupling of Ion Cyclotron Range of Frequencies (ICRF) power to the plasma are greatly influenced by the dynamic behaviour of the plasma layers in front of the antenna. Simulations have shown that the induced RF sheaths contribute to the generation of  $E \times B$  convective transport, impurity generation, hot spots and power dissipation<sup>1</sup>. Even though indirect measurements, such as measuring density and temperature along the toroidal magnetic field lines during ICRF operation, corroborated the simulation results, no direct experimental observation of these effects were available. A new three-strap ICRF antenna was designed for ASDEX Upgrade with the aim of reducing wall W impurity sputtering<sup>2</sup> in a collaboration between IPP, ASIPP and ENEA. This new antenna design also integrates ten small microwave reflectometry antenna pairs (FIG.1), which look at the plasma from different toroidal and poloidal locations<sup>3</sup>.

The new multichannel density profile reflectometry system was designed to use the available embedded antennas to study the evolution of the edge electron density profile at three different poloidal locations directly in front of the ICRF antenna. The new three-strap ICRF

antenna and embedded reflectometry diagnostic were installed successfully on ASDEX Upgrade in 2015. This project was an international collaboration between the ASDEX Upgrade, Germany, ENEA, Italy and Instituto Superior Técnico, Portugal.

## II. REFLECTOMETRY DIAGNOSTIC

The implemented multichannel reflectometry diagnostic was designed to measure edge plasma electron density profiles up to  $2 \times 10^{19} \text{ m}^{-3}$  in X-mode in the typical 1.5 T to 2.7 T magnetic fields of ASDEX Upgrade. The probing wave frequency is swept in the extended U-band between 40 GHz and 68 GHz. This diagnostic uses a modular design, in which the microwave components are physically separated from the host and acquisition systems. This allows the microwave hardware to be attached to the reflectometry antenna waveguides, near the tokamak vessel, while the control and acquisition systems are placed inside the torus hall but kept away from the magnetic interference during the discharge.

The host and control computer is connected to the ASDEX Upgrade network and handles the configuration and data acquisition of the diagnostic. The system integrates a universal time-to-digital converter<sup>4</sup> to generate synchronized triggers for the acquisition and frequency sweep generation. A local solid-state drive temporarily stores the reflectometry raw data files for processing and uploading to the shotfile database. The acquisition system uses the Advanced Telecommunications Computing

---

<sup>a)</sup> Contributed paper published as part of the Proceedings of the 21st Topical Conference on High-Temperature Plasma Diagnostics, Madison, Wisconsin, June, 2016.

<sup>b)</sup> daguiam@ipfn.tecnico.ulisboa.pt

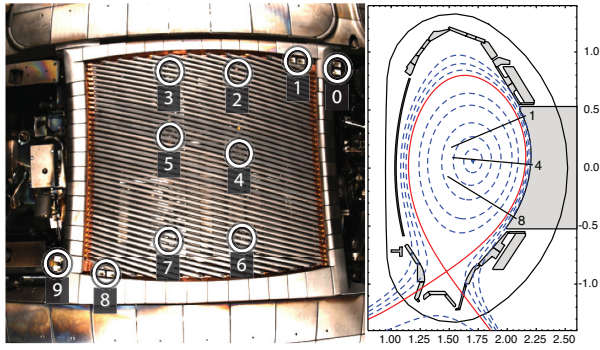


FIG. 1: (Left) ICRF antenna embedded reflectometry antenna locations; (Right) Poloidal cross section of vessel and lines of sight of connected reflectometry antennas 1, 4 and 8.

Architecture standard and communicates with the host computer through a PCI Express link. There are 8 acquisition channels with a 13-bit resolution, a maximum sampling rate of 200 MSamples/s and a total of 512 MB memory per channel<sup>5</sup>. Each reflectometer channel uses two (I and Q) acquisition channels.

In a typical reflectometer operational configuration, the full frequency range is swept in  $15 \mu\text{s}$ , generating a electron density profile every  $100 \mu\text{s}$ . This configuration allows covering 8.9 seconds of the ASDEX Upgrade discharge and is limited by data acquisition system memory. In fast sampling configuration a density profile can be obtained every  $25 \mu\text{s}$  covering around 2.2 s. This mode is used for detailed sampling of fast plasma events.

A total of 10 reflectometry antennas, grouped in pairs of transmitting and receiving antennas, are embedded in the ICRF antenna #4, in sector 12 of ASDEX Upgrade tokamak (see FIG.1). The outer antennas (0, 1, 8, and 9) are pyramidal horn antennas located between the last Faraday straps and the ICRF antenna limiter. The central reflectometer antennas (2-7) have to look through the small gap between the Faraday shield straps, and use WR42 waveguide tapers instead pyramidal horns. The CO12 port vacuum flange allowed the access of only 14 WR19 waveguides, restricting access to only 7 preselected reflectometry antenna pairs at a time without rerouting the in-vessel waveguides. The implemented diagnostic uses three channels, connected to antennas 1, 4 and 8, with the possibility for new channels in future upgrades.

### A. Reflectometer architecture and operation

In the typical operation of a density profile reflectometer, the probing wave propagates in the plasma and is reflected at a cut-off layer where the index of refraction goes to zero, depending on the probing wave frequency and the local plasma characteristics. By sweeping the probing frequency it is possible to estimate the electron density of the plasma layer at which the wave is reflected.

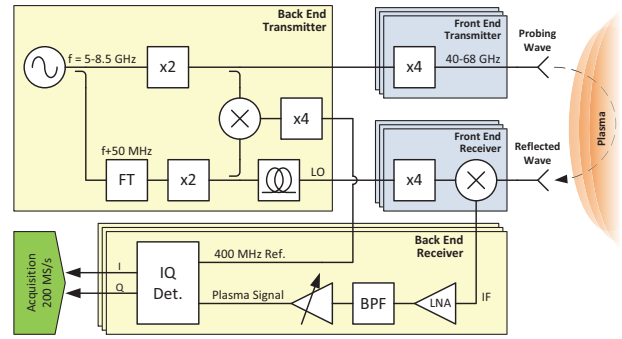


FIG. 2: Heterodyne topology of the reflectometer.

Mixing the reflected wave with a local oscillator signal results in a beat signal whose frequency is proportional to the group delay of the probing wave propagating in the plasma. Density profiles can be measured from almost zero density using the X-mode upper cut-off, up to a maximum density limited by the plasma magnetic field and the quality of the signal near the end of the probing band. This diagnostic uses the full coherent heterodyne architecture (see FIG. 2) that provides in-phase and quadrature (IQ) beat signals for each of the reflectometer channels.

A single Voltage Controlled Oscillator (VCO) is used to generate a 5-8.5 GHz signal, which is split into two branches. In the transmitting branch, this signal is doubled, power split in three and used as the source of each transmitter front-end. Each transmitter front-end consists of an active frequency quadrupler attached directly to the reflectometry transmitting antenna waveguide, providing the 40-68 GHz probing signal with a maximum power output of +16 dBm. In the local oscillator (LO) branch, a frequency translator module introduces a 50 MHz shift in the source signal to generate a coherent 5.05-8.55 GHz reference signal, which is doubled and quadrupled to drive the mixers LO port.

The receiver front-end consists of an active frequency quadrupler and a fundamental mixer. The reflected wave is mixed with the LO signal generating a beat signal, whose frequency is proportional to the delay of the reflected wave, centered at an intermediate frequency of 400 MHz. A coaxial delay line partially compensates the delay introduced by the long waveguide transmission line (about 10 m), and keeps the beat frequency within the IQ detector bandwidth (100 MHz). In the receiver back-end, the beat signal is filtered and amplified. The quadrature detector uses the synchronized reference to demodulate the beat signal into its IQ components, which are then acquired.

The raw IQ signals are then calibrated to remove the effect of waveguide dispersion, which corresponds to an added group delay that decreases non-linearly as a function of the probing wave frequency. A spectral analysis of the signal is performed to determine the start of the plasma reflected signal, which corresponds to the zero

density reflection, known as the first fringe, and can occur anywhere in the 40-68 GHz band, depending on the local magnetic field and the distance of the plasma to the antenna. The measured group delay, the probing wave frequency and the magnetic field profile along the line of sight obtained from the equilibrium codes are then used to invert the density profile<sup>6</sup>.

### III. EXPERIMENTAL RESULTS

For a plasma period with no ICRF heating (#33520 at 3.999 s), the measured group delay for each antenna and the automatically calculated first fringe frequency (dashed line) are shown in FIG. 3 (left). The corresponding density profiles in FIG. 3 (right) are compared with the density profiles obtained with the Lithium Beam and O-mode reflectometry diagnostics. As each diagnostic is located at distinct toroidal and poloidal positions inside the vessel, the profiles are presented in  $\rho_{pol}$  flux coordinates.

A commissioning shot was designed to study the performance of the new reflectometry diagnostic in tracking the density profiles modification during variations of the plasma outer radial position and plasma shape, by changing plasma triangularity, and toggling ICRF heating. The measured radial displacement of the edge isodensity layers in front of each connected antenna, represented in FIG. 4, agrees with the separatrix displacement. Changes in plasma triangularity affect the measurements of the upper (1) and lower (8) antennas. Local effects due to ICRH24 operation can be observed in antenna 1.

### IV. SUMMARY AND CONCLUSIONS

The new multichannel X-mode edge plasma electron density profile reflectometry diagnostic for the ICRF antenna has been successfully installed and commissioned on ASDEX Upgrade, Germany. Changes in the plasma outer radial position and plasma triangularity were observed using the density profiles obtained in front of each

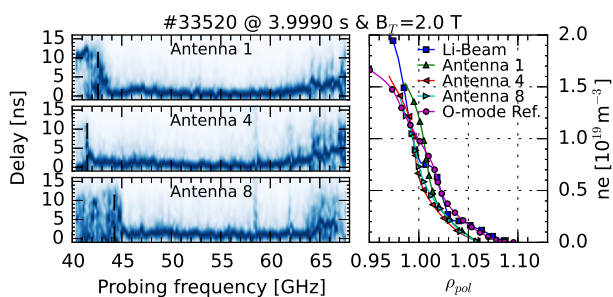


FIG. 3: (Left) Measured reflectometry antenna signal delay and estimated first fringe frequency (dashed line); (Right) Comparison of measured density profiles with other diagnostic data.

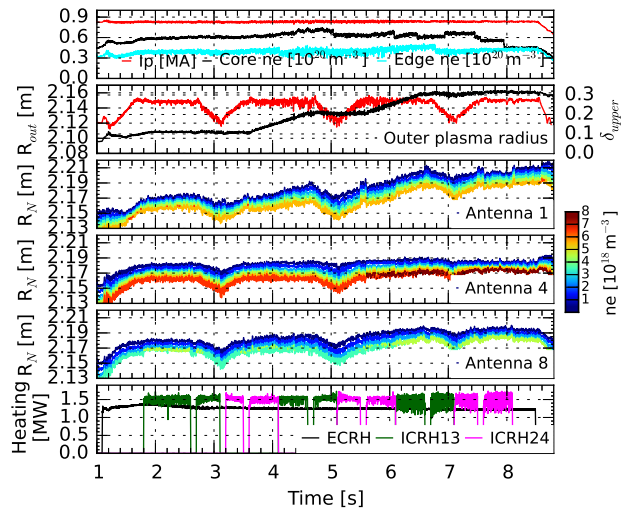


FIG. 4: AUG#33214 Evolution of the measured isodensity lines during a scan of the plasma outer radial position and triangularity with  $B_T=2.5$  T.

antenna location. Early results show that this multichannel reflectometry diagnostic will enhance and improve the analysis of plasma poloidal variations and the observation of convective cells during ICRF operation.

### ACKNOWLEDGMENTS

This work has been carried out within the framework of the EUROfusion Consortium and has received funding from the Euratom research and training programme 2014-2018 under grant agreement No 633053. IST activities also received financial support from Fundação para a Ciência e Tecnologia through project UID/FIS/50010/2013 and the PhD Scholarship FCT-SFRH/BD/52414/2013. The views and opinions expressed herein do not necessarily reflect those of the European Commission.

- <sup>1</sup>D. A. D'Ippolito and J. R. Myra, *Physics of Plasmas* **13** (2006), 10.1063/1.2360507.
- <sup>2</sup>V. Bobkov, M. Balden, R. Bilato, F. Braun, R. Dux, A. Herrmann, H. Faugel, H. Fünfgelder, L. Giannone, A. Kallenbach, H. Maier, H. Müller, R. Neu, J.-M. Noterdaeme, T. Pütterich, V. Rohde, N. Tsujii, F. Zeus, and H. Zohm, *Nuclear Fusion* **53**, 093018 (2013).
- <sup>3</sup>O. Tudisco, A. Silva, S. Ceccuzzi, O. D'Arcangelo, G. Rocchi, H. Fuenfgelder, V. Bobkov, R. Cavazzana, G. D. Conway, J. Friesen, B. Gonçalves, A. Mancini, L. Meneses, J. M. Noterdaeme, G. Siegl, A. Simonetto, N. Tsujii, A. A. Tuccillo, T. Vierle, I. Zammuto, ASDEX Upgrade Team, and FTU Team, *AIP Conference Proceedings* **1580**, 566 (2014).
- <sup>4</sup>G. Raupp, R. Cole, K. Behler, M. Fitzek, P. Heimann, A. Lohs, K. Lüddecke, G. Neu, J. Schacht, W. Treutterer, D. Zasche, T. Zehetbauer, and M. Zilker, *Fusion Engineering and Design* **66-68**, 947 (2003).
- <sup>5</sup>R. C. Pereira, A. M. Fernandes, A. C. Neto, J. Sousa, A. J. Batista, B. B. Carvalho, C. M. B. A. Correia, and C. A. F. Varandas, *IEEE Transactions on Nuclear Science* **57**, 683 (2010).
- <sup>6</sup>E. Mazzucato, *Review of Scientific Instruments* **69**, 2201 (1998).